Optical and Quantum Electronics (2022) 54:595
https://doi.org/10.1007/s11082-022-04004-z

Sensitivity enhancement of refractive index-based surface plasmon resonance sensor for glucose detection

Bhishma Karki[1,2] · Ankit Jha[3] · Amrindra Pal[3] · Vivek Srivastava[4]

Received: 23 March 2022 / Accepted: 13 July 2022 / Published online: 3 August 2022

Abstract
Diabetes is a life-threatening disease caused by excessive glucose intake. The surface plasmon resonance (SPR) based sensor is the most advanced technology for glucose detection. A multilayer SPR-based sensor for detecting glucose in the urine is presented using nanolayers of silver, MXene, ZnO, and graphene over a BK7 prism. The suggested sensor's performance parameters like sensitivity, quality factor, full width half maximum, and signal-to-noise ratio have all been evaluated. In urine samples, the sensitivity for glucose concentration 0–15 mg/dL is evaluated to be 123 deg/RIU, and for 0.625 g/dL concentration, it has been computed as 131 deg/RIU. Likewise, it has been calculated as 126 deg/RIU, 132 deg/RIU, 132.33 deg/RIU, and 133.5 deg/RIU for 1.25 g/dL, 2.5 g/dL, 5 g/dL, and 10 g/dL, respectively. The corresponding computed values for full width half maximum, quality factor are3.35 deg, 3.37 deg, 3.39 deg, 3.41 deg, 3.48 deg, 3.64 deg and 36.6 RIU^{-1},38.7 RIU^{-1}, 37 RIU^{-1}, 38.6 RIU^{-1}, 37.9 RIU^{-1}, 37.4 RIU^{-1} respectively. The proposed SPR sensor's improved performance makes it a good structure for detecting glucose in urine samples, expanding its application in the medical industry.

Keywords Sensitivity · Surface plasmon resonance · Glucose detection · MXene · ZnO · Graphene

1 Introduction

A surface plasmon (SP) is an electromagnetic charge cloud that originates at the thin metal–dielectric interface and this metal layer's surface (Kim et al. 2019). The transverse magnetic (TM) polarized wave is aimed at a specific incident angle on a metal layer. When

✉ Bhishma Karki
magnum.photon@gmail.com

1 Department of Physics, Tri-Chandra Multiple Campus, Tribhuvan University, Kathmandu 44600, Nepal

2 National Research Council Nepal, New Baneshwor-10, Kathmandu 44600, Nepal

3 Department of ECE, DIT University, Dehradun 248009, India

4 Department of Mechanical Engineering, ABES Engineering College, Ghaziabad, UP 201009, India

the momentum of the incident light equals that of the surface plasmon, a resonance condition is achieved. This phenomenon is known as surface plasmon resonance (SPR). The wave vectors of these two waves are called evanescent wave vector (EWV) and surface plasmon wave vector (SPWV) (Pal and Jha 2021).

The angle at which this resonance condition happened is called the SPR angle. This resonance angle varies with the concentration of the target analytes when biomolecules stick to the metal surface (Liedberg 1983). Quantitative response, label-free sensing, and extensive use in research disciplines are advantages of adopting SPR-based biosensors. (Shankaran et al. 2007). The applications in the field of environmental monitoring (Hu et al. 2009), food safety (Neethirajan et al. 2018), biomedical (Sathya 2021), and pharmacological (Ouyang et al. 2016) make SPR-based sensors useful.

Optical detection approaches are cost-effective and provide a straightforward output format (Ouyang et al. 2017). Several optical glucose sensing systems based upon the plasmon resonance mechanism have been developed in the last decade. The popular Otto (Otto 1968) and Kretschmann (Kretschmann and Raether 1968) design configurations of SPR sensors have been employed mostly in the SPR sensors. With the upper hand of Kretschmann configuration over Otto configuration with its ease of implementation, it is generally preferred (Singh et al. 2021). In the conventional Kretschmann design, a single layer of metal is deposited over the coupling prism. An air gap exists between the coupling prism and the metal in the Otto configuration. Silver-based SPR biosensors provide a steep SPR curve, allowing great selectivity and sensitivity in SPR imaging detection. However, a major disadvantage of silver films in SPR biosensors is their susceptibility to oxidation (Karki et al. 2022).

Several durable metallic or dielectric coatings have been developed to avoid silver from oxidation (Sathya et al. 2022) as a protective layer to diminish the effect of oxidation as potential material graphene has been considered. A single graphene layer is about 0.34 nm thick, and with its hexagonal ring-type structure, the molecules cannot pass through due to its high electron density. Hence, this property of graphene makes it a perfect candidate for protecting metal surfaces against corrosion. Other than these, its other physiochemical properties include high surface area, higher electrical conductivity, mechanical strength, and greater thermal conductivity with ease of surface functionalization (Sungjin Park et al. 2008)-(Georgakilas et al. 2012).

Another 2D material, MXene, has been employed in our proposed design due to its attractive properties, including its layered morphology, greater electrical conductivity and surface area, high hydrophilicity, and thermally stable (Pandey et al. 2021). Previous work, which includes nanolayers of MXene ($Ti_3C_2T_x$) and gold (Au), has been employed for glucose detection (Rakhi et al. 2016).

Besides these materials, an additional metal-oxide nanolayer of ZnO has also been employed in the proposed design. This layer acts as an adhesive layer. Its attractive properties like a wide bandgap of 3.37 eV (Mudgal et al. 2020a), greater exciton energy of 60 meV (Guo et al. 2020), and not costly make it suitable for sensing-based applications. Moreover, ZnO with metals (Ag or Au) is generally employed in the prism-based SPR sensors for performance enhancement (Mei and Menon 2020).

For the human body, glucose is an important source of energy. Excessive intake may adversely affect many human body parts like the heart, kidney, and eyes. (Mudgal et al. 2020b). Diabetes is a very common disease caused due to excessive glucose intake. Globally, around 422 million people were affected, and above 1.6 million died, according to the World Health Organization (WHO) report (Mostufa et al. 2021). In urine, enhanced glucose concentration causes Renal glycosuria (Karim et al. 2018). So, the detection of

Glucose concentration is required to prevent a kidney relied disease. The variation in the RI of the urine sample of an affected person from an average healthy person due to glucose concentration is always being noted. The unit of glucose concentration is expressed in mg per deciliter(mg/dl). Normally, the range of 0 to 15 mg/dL glucose concentration in the human body is absent. The condition of renal glycosuria generally rises as the glucose levels rise in the urine samples (in the range of 165 mg/dl to 180 mg/dl. Based on the glucose concentration levels, two conditions have been classified: Hypoglycemia (for lower concentration levels) and Hyperglycemia (for higher concentration levels). Hypoglycemia indicates the glucose concentration smaller than 40 mg/dL and hyperglycemia indicates 279–360 mg/dL range (Sani and Khosroabadi 2020).

This research manuscript is categorized into different sections. This section sets up an introductory part of SPR sensors, followed by Sect. 2 (which explains the designing and modeling part of the proposed sensor). Then, Sect. 3 gives the results and discussions of our research. At last, followed by the conclusion in Sect. 4.

2 Sensor designing and modelling

The proposed SPR sensor design consists of a single silver metal layer (40 nm); above it, a layer of MXene (0.993 nm) is placed, followed by ZnO (2 nm), graphene (0.34 nm), and sensing layers. The proposed sensor is shown in Fig. 1.

An input optical wave gets generated with the He–Ne laser source. With this source, a transverse magnetic (p-polarized) wave is incident on the part of the BK7 (borosilicate) prism, and the wave reflected comes out of another surface. The principle is followed by the incident wave known as attenuated total reflection (ATR) (Homola 2008). The surface plasmon generally gets excited using a low RI coupling prism. The reason behind this is the balance condition between SPWV and EWV. The upcoming Table 1 summarizes the design parameters for different sensor layers.

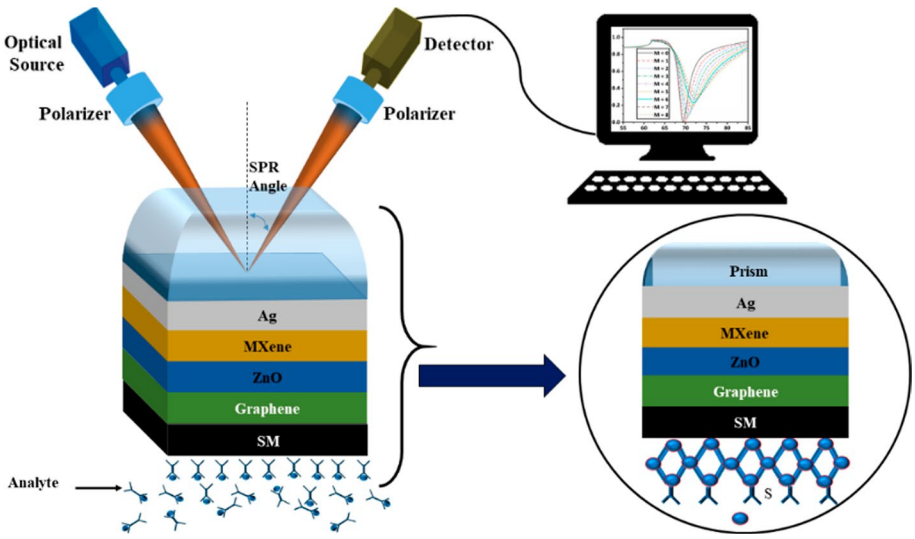

Fig. 1 The proposed five-layer schematic diagram for SPR sensor design for glucose detection

Table 1 Different layers parameters

Layer	Materials (base as BK7 Prism)	Thickness (in nm)	R.I. at 633 nm
1	Silver, Ag	$D_1 = 40$	$0.056206 + i * 4.2776$
2	MXene	$D_2 = M * 0.993$	$2.38 + i * 1.33$
3	Zinc oxide (ZnO)	$D_3 = 2$	1.9576
4	Graphene	$D_4 = G * 0.343$	$+ \mathrm{i} * 1.1491$
5	Sensing medium	–	$1.33 + \Delta$ n

The RI of the BK7 prism is being calculated using Sellmeier equation (Jabin, et al. 2019):

$$\mathrm{n_{BK7}} = \left(\frac{\alpha_a \lambda^2}{\lambda^2 - \beta_a} + \frac{\alpha_b \lambda^2}{\lambda^2 - \beta_b} + \frac{\alpha_c \lambda^2}{\lambda^2 - \beta_c} + 1 \right)^{1/2} \tag{1}$$

The constants α_a, α_b, α_c have the values.

For silver metal, its R.I. is computed using Drude Lorentz model (Singh and Raghuwanshi 2021):

$$\mathrm{n_{Ag}} = \left(1 - \frac{\lambda^2 * \lambda_c}{\lambda_p^2 (\lambda_c + \lambda * \mathrm{i})} \right)^{1/2} \tag{2}$$

where the values of λ_c (collision wavelength) is $8.9342 * 10^{-6}$ m and λ_p (plasma wavelength) is $1.6826 * 10^{-7}$ m.

For computing the reflectance, the transfer matrix method is employed (Uniyal et al. 2022a). For this, a **c**haracteristic matrix has been used to define the N-layer structure, as shown in Eq. 3.

$$\mathrm{T} = \prod_{\mathrm{K}}^{\mathrm{N}-1} \mathrm{T_K} = \begin{bmatrix} \mathrm{T_{11}} & \mathrm{T_{12}} \\ \mathrm{T_{21}} & \mathrm{T_{22}} \end{bmatrix} \tag{3}$$

as

$$\mathrm{T_K} = \begin{bmatrix} \cos\beta_k & -\mathrm{i}\sin(\beta_k / q_k) \\ -\mathrm{i} q_k \sin\beta_k & \cos\beta_k \end{bmatrix} \tag{4}$$

here, $\mathrm{T_K}$ is the kth layer matrix, β_k isthe optical admittance and q_k is the phase factor.

$$\beta_k = \frac{2\pi}{\lambda} d_k \sqrt[2]{\epsilon_k - n_1^2 \sin^2\theta_1}$$

$$q_k = \sqrt[2]{\epsilon_k - n_1^2 \sin^2\theta_1} \Big/ \epsilon_k$$

Here, θ_1 is the angle of incidence and ϵ_k is the dielectric constant.

The coefficients of reflection of p-polarized (TM mode) incident wave are expressed as:

$$R_p = \left|r_p\right|^2 = \left(\frac{(T_{11} + T_{12}q_N)q_1 - (T_{21} + T_{22}q_N)}{(T_{11} + T_{12}q_N)q_1 + (T_{21} + T_{22}q_N)}\right) \tag{5}$$

The proposed structure can be fabricated using the following fabrication steps. Initially, the acetone vapor, methanol, and deionized water solution were first applied to the coupling glass prism before being coupled to the silver nanolayer. A thermal evaporator apparatus is used for physical vapor deposition (PVD) of silver layers over the prism glass (Luna-Moreno et al. 2020). The liquid exfoliation method could be used to prepare the MXene layer and chemically shift it over the silver nanolayer. The fabrication of the graphene nanolayer was performed using the Chemical vapor deposition (CVD) process (Kumar et al. 2020) and transferred over the ZnO layer, which can be prepared using electro-chemical deposition (Atiq, et al. 2020).

At last, the chip is kept over the BK7 prism. The simulated experimental results are computed using a sensor setup for sensing purposes, a deionized aqueous solution containing bacteria and viruses. This mixture is also poured over an SPR sensor chip through an input flow cell for the biomolecular reaction between an analyte and basic recognition element (BRE). The input monochromatic radiation of 633 nm wavelength falls on one side of BK7 prism after passing through the polarizer stage. An optical photodetector detects the reflected radiation, and the final output signal strength is directly proportional to the reflected light intensity.

2.1 Performance parameters defining sensor performance

The performance analysis of a sensor has been computed with the help of parameters like sensitivity (S), full-width half maximum (FWHM), quality factor (QF), and signal-to-noise ratio (SNR). The values for S, QF, and DA must be high for better performance of the proposed sensor with the low value of FWHM (Mohanty et al. 2016).

2.2 Sensitivity (denoted by S)

It is defined as the ratio of the deviation in the SPR angle ($\Delta\theta_{res}$) and the deviation in the sensing medium's RI (Δn). It is mathematically expressed as:

$$S = \frac{\Delta\theta_{res}}{\Delta n}(\text{in deg/RIU}) \tag{6}$$

2.3 Full width half maxima (denoted by FWHM)

This parameter gives information about the width and sharpness of the reflectance curve. It is mathematically expressed as:

$$\text{FWHM} = \theta_2 - \theta_1(\text{in deg}) \tag{7}$$

Here, θ_2 *and* θ_1 indicates the difference between incidence angles at half (50%) of reflectivity.

2.4 Quality factor (denoted by QF)

This parameter gives information about the resolution of the proposed SPR sensor. It is mathematically expressed with the relation:

$$\mathrm{QF} = \mathrm{S}/\mathrm{FWHM}\left(\text{in RIU}^{-1}\right) \tag{8}$$

2.5 Signal to noise ratio (denoted by SNR)

It is the inverse of FWHM. This factor is determined using the SPR curve. It is mathematically expressed as:

$$\mathrm{SNR} = 1/\mathrm{FWHM}\left(\text{in deg}^{-1}\right) \tag{9}$$

2.6 Field distribution computation

The field distribution of the input TM polarized wave within each layer of our proposed sensor design indicates the evanescent field augmentation with various conditions. The evanescent field's production over the analysis interface is critical for the surface plasmon resonance mechanism, as the sensing is to be done on this analyte's interface. So, using the expression of the total characteristics matrix, the field components distribution with the first layer can be expressed as (Shalabney and Abdulhalim 2010) (Uniyal et al. 2022b):

$$\begin{bmatrix} \mathrm{H_{y1}(z)} \\ -\mathrm{E_{x1}(z)} \end{bmatrix} = \mathrm{P_1(z)}.\begin{bmatrix} 1+\mathrm{r_p} \\ \mathrm{q_1}(1-\mathrm{r_p}) \end{bmatrix}\mathrm{H_y^{inc}}, \mathrm{z_1} \le \mathrm{z} \le \mathrm{z_2} \tag{10}$$

Here, $\mathrm{H_{y1}(z)}, \mathrm{E_{x1}(z)}$ are magnetic field and electric field, respectively.
$\mathrm{H_y^{inc}}$ indicates incident magnetic field amplitude and $\mathrm{r_p}$ is the reflection coefficient.
here,

$$\mathrm{P_1(z)} = \begin{bmatrix} \cos(\beta_{\mathrm{k(atz)}}) & \mathrm{i}/\mathrm{q_1}\sin(\beta_{\mathrm{k(atz)}}) \\ \mathrm{iq_1}\sin(\beta_{\mathrm{k(atz)}}) & \cos(\beta_{\mathrm{k(atz)}}) \end{bmatrix} \tag{11}$$

Next, these field distributions within the layer $\mathrm{j} \ge 2$ are given by:

$$\begin{bmatrix} \mathrm{H_{yj}(z)} \\ -\mathrm{E_{xj}(z)} \end{bmatrix} = \mathrm{P_j(z)} * \prod_{\mathrm{j-1}}^{1} \mathrm{P(z = z_i + d_i)} * \begin{bmatrix} 1+\mathrm{r_p} \\ \mathrm{q_j}(1-\mathrm{r_p}) \end{bmatrix}\mathrm{H_y^{inc}}, \mathrm{z_j} \le \mathrm{z} \le \mathrm{z_{j+1}} \tag{12}$$

here,

$$\text{Propagation matrix}, \mathrm{P_j(z)} = \begin{bmatrix} \cos(\beta_{\mathrm{k(atz=z-1)}}) & \mathrm{i}/\mathrm{q_j}\sin(\beta_{\mathrm{k(atz=z-1)}}) \\ \mathrm{iq_j}\sin(\beta_{\mathrm{k(atz=z-1)}}) & \cos(\beta_{\mathrm{k(atz=z-1)}}) \end{bmatrix} \tag{13}$$

3 Results and discussions

For the four different MXene and graphene layers combinations, the SPR reflectance plots were plotted for two different RI of 1.335 and 1.336 (Fig. 2). The RI alteration was taken as 0.001.

Figure 2a indicates the SPR curves for the traditional SPR sensor design (i.e., for $M = 0,\ G = 0$). The M and G here indicate the number of MXene and graphene layers. The sensitivity computed for this traditional design is $S = 123$ deg/RIU—the SPR curve shifts to a higher angle of incidence. Figure 2b indicates the SPR reflectance curve for $M = 0,\ G = 1$. The corresponding sensitivity value for this modified traditional design computed is $S = 124$ deg/RIU. For the next cases of $M = 1,\ G = 0$ (shown in Fig. 2c) and $M = 1, G = 1$ (shown in Fig. 2d), the values computed for sensitivity are 131 deg/RIU and 139 deg/RIU. The inclusion of both layers of MXene and graphene greatly improves the sensitivity as compared to the traditional design.

3.1 Layer optimization

In the optimized layer, we get the minimum reflectance of 40 nm for Ag metal. Figure 3 shows the reflectance as a function of the angle of incidence plot. The different thicknesses of silver metal taken here are 30 nm, 35 nm, 40 nm, 45 nm, and 50 nm for finding the

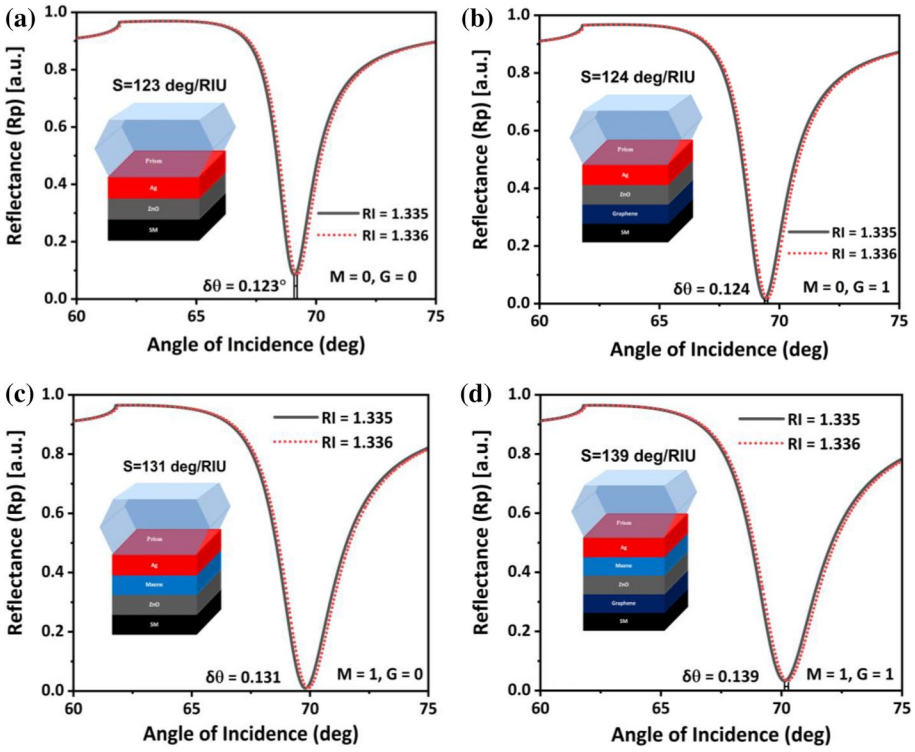

Fig. 2 The SPR curves for **a** $M = 0, G = 0$, **b** $M = 0, G = 1$, **c** $M = 1, G = 0$, and **d** $M = 1, G = 1$

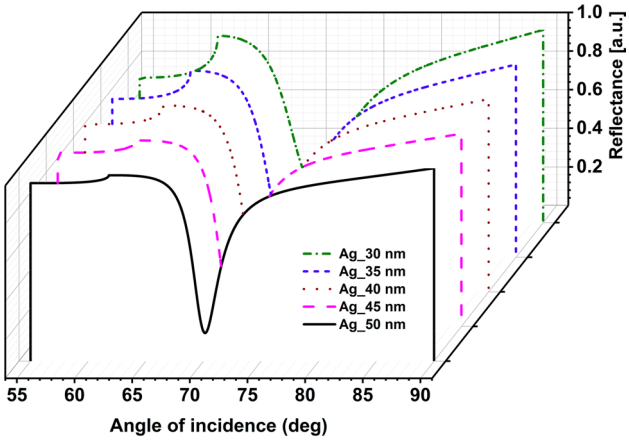

Fig. 3 Reflectance plots for silver layer thickness (from 30 to 50 nm)

optimized metal layers thickness. Table 2 shows the corresponding minimum reflectance values for different thicknesses of the silver metal layer.

The minimum reflectance value of 0.001 has been computed for the silver layer thickness of 40 nm.

With variation in the number of MXene layers from 0 to 3 keeping the graphene layer constant (equal to 1), the variation in SPR curve widths has been observed (Fig. 4a). The width of the SPR curve increases with an increased angle of incidence. Figure 4b shows the SPR curve variations for different graphene layers from 0 to 7. The value of minimum reflectance increases rapidly with increasing the number of graphene layers taking a single MXene layer (Table 3).

3.2 Glucose detection

Suppose the patient has diabetes and the glucose level in their urine changes. Similarly, we must place biological urine samples on the surface of the graphene layer to detect glucose levels in urine samples. The sensor would detect a refractive index increase due to increased glucose concentration levels in urine samples by moving the SPR angle to the right. Table 4 shows how the RI changes as the glucose concentration vary, determining a urine sample's glucose levels. Figure 5 depicts the SPR curves for detecting glucose in urine samples. As glucose concentration in urine samples rises, the refractive index rises, causing an SPR angle shift. For RI change of 0.001, the maximum sensitivity

Table 2 Silver layer thickness with corresponding minimum reflectance

Ag metal layer thickness	Minimum reflectance
30 nm	0.205
35 nm	0.065
40 nm (optimized)	0.001
45 nm	0.033
50 nm	0.146

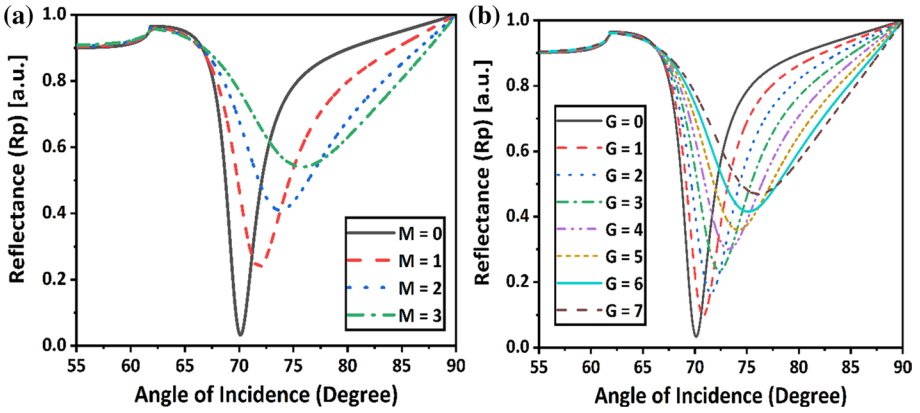

Fig. 4 Reflectance variation with increasing angle of incidence for **a** MXene layers variation 0 to 3, **b** graphene layers variation from 0 to 7

Table 3 Detecting the levels of glucose using urine samples

Glucose concentration	RI	Δ RI	θ_{SPR}	$\Delta\theta_{SPR}$(deg)	Min. Reflectance	S (deg/RIU)
0 – 15 mg/dL	1.335	*ref*	70.118	*ref*	0.03305	*ref*
0.625 g/dL	1.336	0.001	70.249	0.131	0.03323	131
1.25 g/dL	1.337	*ref*	70.375	0.126	0.03343	126
2.5 g/dL	1.338	0.001	70.507	0.132	0.03363	132
5 g/dL	1.341	*ref*	70.904	0.397	0.03429	132.33
10 g/dL	1.347	0.006	71.723	0.819	0.03592	136.5

Table 4 Performance parameters computation of proposed SPR sensor

RI	Sensitivity (deg/RIU)	FWHM (deg)	QF (RIU^{-1})	SNR (deg^{-1})
1.335	123	3.35	36.6	0.298
1.336	131	3.37	38.7	0.296
1.337	126	3.39	37	0.294
1.338	132	3.41	38.6	0.293
1.341	132.33	3.48	37.9	0.287
1.347	136.5	3.64	37.4	0.274

calculated is 132 deg/RIU, minimum reflectance of 0.03305 has been observed. Next, for 0.006 RI change, the maximum value sensitivity calculated is 136.5 deg/RIU (for 10 g/L), minimum reflectance of 0.03429 has been observed. For glucose concentration variation from 0 – 15 mg/dL to2.5 g/dL, the angle of incidence shifts to 70.507 Degree from 70.118 Degree for 0.001 RI variation. In a similar manner for RI change of 0.006, the angle of incidence shifted to 71.723 Degree.

The output detector detects a change in SPR angle due to a change in glucose concentration, allowing the glucose level to be reliably detected in urine samples.

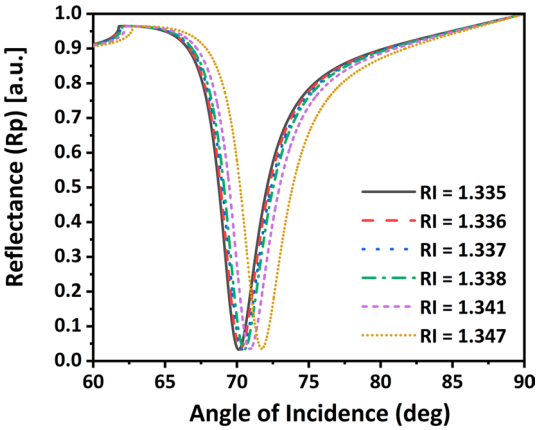

Fig. 5 Glucose level detection with RI fluctuations in urine samples

The upcoming table, Table 4, gives the performance parameters computed for the proposed sensor.

3.3 Field intensity plot

For the proposed SPR sensor design, the electric field intensity values for different interfaces regarding the normal distance from the prism interface have been plotted in Fig. 6. The electric field intensity is maximum at the last interface of the graphene layer. This is due to the stronger excitation of surface plasmons at this interface**.**

A comparison is made with the earlier research in SPR sensors. This comparison has been shown with the help of Table 5.

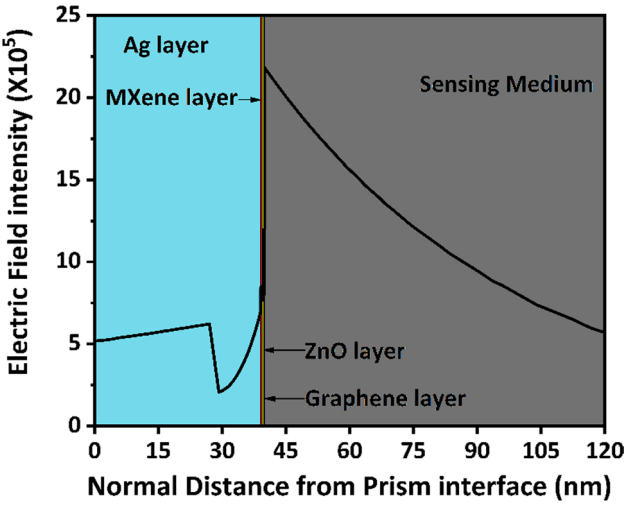

Fig. 6 Electric field distribution for proposed SPR sensor

Table 5 Comparison between the present sensor and earlier reported sensors

Design layers	Operating wavelength	QF	SNR	S	References
Prism/Ag/MXene/ZnO/Graphene	633 nm	38.7	0.298	136.5	Proposed
Prism/ZnO/Ag/Au/BaTiO3/Graphene	632.8 nm	37.87	4.54	116.67	Mudgal et al. (2020a)
Prism/ZnO/Au/MoS2/Graphene	632.8 nm	15.11	1.81	101.58	Kushwaha et al. (2018)
Prism/Au/MoS2/Graphene	633 nm	17.56	1.28	87.80	Rahman et al. (2017)
Prism/Ag/graphene	633 nm	52.31	–	91.76	Maharana et al. (2013)

4 Conclusion

An SPR-based sensor has been proposed to measure the glucose concentration in human urine samples. Glucose sensing is relied on measuring the urine sample's RI. The Kretschmann configuration using the attenuated total reflection principle is employed for detection. The performance parameters such as sensitivity, FWHM, QF, and SNR have been computed, showing the performance of the proposed structure. The observed values for the proposed glucose detection SPR sensor for sensitivity, FWHM, QF, and SNR are 136.5 deg/RIU, 3.35 degree, 38.7 RIU^{-1},0.298 degree − 1. These enhanced performance parameters open the gate for this proposed design in sensing-based applications.

Acknowledgements The authors are thankful to Dr. Aman Jha and Dr. Nivedita Jha, founder of K. K. Dental care, for supporting the research work.

Author contributions BK: formulated the problem statement, giving the theoretical background and mathematical modeling for the SPR biosensor. He also helped in drafting and finalizing the manuscript. AJ: provided the theoretical background to biosensing and the importance of Optical Biosensing. He also helped in finalizing the design of the proposed sensor. AP: worked towards the complete manuscript, formatting, and finalizing the manuscript. VS: provided statistical analysis for the results. He provided the theoretical background to SPR biosensors. He also helped in formatting the manuscript.

Funding None.

Declarations

Conflict of interest The author declares that he has no conflict of interest.

Consent to participate I am willing to participate in the work presented in this manuscript.

Consent for publication The author has given their consent to publish this work.

Ethical approval Not applicable. The work presented in this manuscript is mathematical modeling only for the proposed biosensor. No experiment was performed on the human body and living organism/ animal. So, ethical approval from an ethical committee is not required.

References

Asaduzzaman Jabin, M.A., et al.: Surface plasmon resonance based titanium coated biosensor for cancer cell detection. IEEE Photonics J. **11**(4), 1–10 (2019). https://doi.org/10.1109/JPHOT.2019.2924825

Georgakilas, V., et al.: Functionalization of graphene: Covalent and non-covalent approach. Chem. Rev. **112**(11), 6156–6214 (2012)

Guo, S., Wu, X., Li, Z., Tong, K.: High-sensitivity biosensor-based enhanced SPR by ZnO/MoS2Nanowires array layer with graphene oxide nanosheet. Int. J. Opt. **2020**, 1–6 (2020). https://doi.org/10.1155/2020/7342737

Homola, J.: Surface plasmon resonance sensors for detection of chemical and biological species. Chem. Rev. **108**(2), 462–493 (2008). https://doi.org/10.1021/cr068107d

Hu, C., Gan, N., Chen, Y., Bi, L., Zhang, X., Song, L.: Detection of microcystins in environmental samples using surface plasmon resonance biosensor. Talanta **80**(1), 407–410 (2009). https://doi.org/10.1016/j.talanta.2009.06.044

Karim, M.N., Anderson, S.R., Singh, S., Ramanathan, R., Bansal, V.: Nanostructured silver fabric as a free-standing NanoZyme for colorimetric detection of glucose in urine. Biosens. Bioelectron. **110**, 8–15 (2018). https://doi.org/10.1016/j.bios.2018.03.025

Karki, B., Uniyal, A., Chauhan, B., Pal, A.: Sensitivity enhancement of a graphene, zinc sulfide-based surface plasmon resonance biosensor with an Ag metal configuration in the visible region. J. Comput. Electron. **21**(2), 445–452 (2022). https://doi.org/10.1007/s10825-022-01854-4

Kim, N.-H., Choi, M., Kim, T.W., Choi, W., Park, S.Y., Byun, K.M.: Sensitivity and stability enhancement of surface plasmon resonance biosensors based on a large-area Ag/MoS2 substrate. Sensors **19**(8), 1894 (2019). https://doi.org/10.3390/s19081894

Kretschmann, E., Raether, H.: Radiative decay of non-radiative surface plasmons by light. Z. Naturforsch **23**(a), 2135–2136 (1968)

Kumar, A., et al.: A comparative study among WS 2, MoS 2 and graphene based surface plasmon resonance (SPR) sensor. Sens. Actuators Rep. **2**(1), 100015 (2020). https://doi.org/10.1016/j.snr.2020.100015

Kushwaha, A.S., Kumar, A., Kumar, R., Srivastava, S.K.: A study of surface plasmon resonance (SPR) based biosensor with improved sensitivity. Photonics Nanostruct.-Fundam. Appl. **31**(June), 99–106 (2018). https://doi.org/10.1016/j.photonics.2018.06.003

Liedberg, B.: Surface plasmon resonance for gas detection and biosensing*. Sens. Actuators **4**, 299–304 (1983)

Luna-Moreno, D., Sánchez-Álvarez, A., Rodríguez-Delgado, M.: Optical thickness monitoring as a strategic element for the development of SPR sensing applications. Sensors (Switzerland) **20**(7), 1807 (2020). https://doi.org/10.3390/s20071807

Maharana, P.K., Padhy, P., Jha, R.: On the field enhancement and performance of an ultra-stable SPR biosensor based on graphene. IEEE Photonics Technol. Lett. **25**(22), 2156–2159 (2013)

Mei, G.S., Susthitha Menon, P., Hegde, G.: ZnO for performance enhancement of surface plasmon resonance biosensor: a review. Mater. Res. Express **7**(1), 012003 (2020). https://doi.org/10.1088/2053-1591/ab66a7

Mohanty, G., Akhtar, J., Sahoo, B.K.: Effect of semiconductor on sensitivity of a graphene-based surface plasmon resonance biosensor. Plasmonics **11**(1), 189–196 (2016). https://doi.org/10.1007/s11468-015-0033-0

Mostufa, S., Paul, A.K., Chakrabarti, K.: Detection of hemoglobin in blood and urine glucose level samples using a graphene-coated SPR based biosensor. OSA Contin. **4**(8), 2164 (2021). https://doi.org/10.1364/osac.433633

Mudgal, N., Saharia, A., Agarwal, A., Singh, G.: ZnO and Bi-metallic (Ag–Au) layers based surface plasmon resonance (SPR) biosensor with BaTiO3 and graphene for biosensing applications. IETE J. Res. (2020a). https://doi.org/10.1080/03772063.2020.1844074

Mudgal, N., Saharia, A., Agarwal, A., Ali, J., Yupapin, P., Singh, G.: Modeling of highly sensitive surface plasmon resonance (SPR) sensor for urine glucose detection. Opt. Quantum Electron. **52**(6), 1–14 (2020b). https://doi.org/10.1007/s11082-020-02427-0

Neethirajan, S., Ragavan, V., Weng, X., Chand, R.: Biosensors for sustainable food engineering: challenges and perspectives. Biosensors **8**(1), 23 (2018). https://doi.org/10.3390/bios8010023

Otto, A.: Excitation of nonradiative surface plasma waves in silver by the method of frustrated total reflection. Z. Für Phys. **216**(4), 398–410 (1968). https://doi.org/10.1007/BF01391532

Ouyang, Q., et al.: Sensitivity enhancement of transition metal dichalcogenides/silicon nanostructure-based surface plasmon resonance biosensor. Sci. Rep. **6**(March), 1–13 (2016). https://doi.org/10.1038/srep28190

Ouyang, Q., et al.: Two-dimensional transition metal dichalcogenide enhanced phase-sensitive plasmonic biosensors: theoretical insight. J. Phys. Chem. C **121**(11), 6282–6289 (2017). https://doi.org/10.1021/acs.jpcc.6b12858

Pal, A., Jha, A.: A theoretical analysis on sensitivity improvement of an SPR refractive index sensor with graphene and barium titanate nanosheets. Optik **231**, 166378 (2021). https://doi.org/10.1016/j.ijleo.2021.166378

Pandey, P.S., Singh, Y., Raghuwanshi, S.K.: Theoretical analysis of the LRSPR sensor with enhance FOM for low refractive index detection using mxene and fluorinated graphene. IEEE Sens. J. **21**(21), 23979–23986 (2021). https://doi.org/10.1109/JSEN.2021.3112530

Rahman, M.S., Anower, M.S., Hasan, M.R., Hossain, M.B., Haque, M.I.: Design and numerical analysis of highly sensitive Au-MoS2-graphene based hybrid surface plasmon resonance biosensor. Opt. Commun. **396**(March), 36–43 (2017). https://doi.org/10.1016/j.optcom.2017.03.035

Rakhi, R.B., Nayuk, P., Xia, C., Alshareef, H.N.: Novel amperometric glucose biosensor based on MXene nanocomposite. Sci. Rep. **6**(October), 1–9 (2016). https://doi.org/10.1038/srep36422

Sathya, N., Karki, B., Rane, K. P., Jha, A., Pal, A.: Tuning and sensitivity improvement of bi-metallic structure-based surface plasmon resonance biosensor with 2-D ξ-Tin Selenide nanosheets. pp. 1–14 (2021) [Online]. Available:http://europepmc.org/article/ppr/ppr370506

Sathya, N., Karki, B., Rane, K. P., Jha, A., Pal, A.: Tuning and sensitivity improvement of bi-metallic structure-based surface plasmon resonance biosensor with 2-D ξ-Tin Selenide nanosheets. Plasmonics **17,** 1001–1008 (2022). https://doi.org/10.1007/s11468-021-01565-9

Sani, M.H., Khosroabadi, S.: A novel design and analysis of high-sensitivity biosensor based on nano-cavity for detection of blood component, diabetes, cancer and glucose concentration. IEEE Sens. J. **20**(13), 7161–7168 (2020). https://doi.org/10.1109/JSEN.2020.2964114

Shahid Atiq, M., et al.: Interlayer effect on photoluminescence enhancement and band gap modulation in Ga-doped ZnO thin films. Superlattices Microstruct. **144**, 106576 (2020). https://doi.org/10.1016/j.spmi.2020.106576

Shalabney, A., Abdulhalim, I.: Electromagnetic fields distribution in multilayer thin film structures and the origin of sensitivity enhancement in surface plasmon resonance sensors. Sens. Actuators, A Phys. **159**(1), 24–32 (2010). https://doi.org/10.1016/j.sna.2010.02.005

Shankaran, D.R., Gobi, K.V., Miura, N.: Recent advancements in surface plasmon resonance immunosensors for detection of small molecules of biomedical, food and environmental interest. Sens. Actuators, B Chem. **121**(1), 158–177 (2007). https://doi.org/10.1016/j.snb.2006.09.014

Singh, Y., Paswan, M.K., Raghuwanshi, S.K.: Sensitivity Enhancement of SPR Sensor with the black phosphorus and graphene with Bi-layer of gold for chemical sensing. Plasmonics **16**(5), 1781–1790 (2021). https://doi.org/10.1007/s11468-020-01315-3

Singh, Y., Raghuwanshi, S.K.: Titanium dioxide (TiO2) coated optical fiber-based SPR sensor in near-infrared region with bimetallic structure for enhanced sensitivity. Optik (stuttg) **226**(P1), 165842 (2021). https://doi.org/10.1016/j.ijleo.2020.165842

Sungjin Park, M.D.S., Zhu, Y., An, J., Ruoff, R.S.: Graphene-based ultracapacitors. Nano Lett. **8**(10), 3498–3502 (2008). https://doi.org/10.1021/acs.langmuir.6b03602

Uniyal, A., Chauhan, B., Pal, A., Singh, Y.: Surface plasmon biosensor based on Bi 2 Te 3 antimonene heterostructure for the detection of cancer cells. Appl. Opt. **61**(13), 3711–3719 (2022a)

Uniyal, A., Chauhan, B., Pal, A., Srivastava, V.: InP and graphene employed surface plasmon resonance sensor for measurement of sucrose concentration : a numerical approach. Opt. Eng. **61**(May), 1–13 (2022b). https://doi.org/10.1117/1.OE.61.5.057103